

## Article

# Interannual Variability of Air Temperature over Myanmar: The Influence of ENSO and IOD

Zin Mie Mie Sein <sup>1</sup>, Irfan Ullah <sup>2</sup> , Sidra Syed <sup>3</sup>, Xiefei Zhi <sup>4,5,\*</sup>, Kamran Azam <sup>6</sup> and Ghulam Rasool <sup>1,7</sup> 

- <sup>1</sup> Binjiang College, Nanjing University of Information Science and Technology, Wuxi 214105, China; dr.zin28@gmail.com (Z.M.M.S.); grasool@zju.edu.cn (G.R.)
  - <sup>2</sup> School of Atmospheric Science, Nanjing University of Information Science and Technology (NUIST), Nanjing 210044, China; irfan.marwat@nuist.edu.cn
  - <sup>3</sup> Institute of Peace and Conflicts Studies, University of Peshawar, 25000 Peshawar, Pakistan; sidsyed.92@yahoo.com
  - <sup>4</sup> Key Laboratory of Meteorological Disasters, Ministry of Education (KLME)/Collaborative Innovation Center on Forecast and Evaluation of Meteorological Disasters (CIC-FEMD), Nanjing University of Information Science and Technology, Nanjing 210044, China
  - <sup>5</sup> Weather Online Institute of Meteorological Applications, Wuxi 214000, China
  - <sup>6</sup> Department of Management Sciences, University of Haripur, 22780 Khyber Pakhtunkhwa, Pakistan; kamranazamkhan@yahoo.com
  - <sup>7</sup> School of Mathematical Sciences, Zhejiang University, Hangzhou 310027, China
- \* Correspondence: zhi@nuist.edu.cn

**Abstract:** Myanmar is located in a tropical region where temperature rises very fast and hence is highly vulnerable to climate change. The high variability of the air temperature poses potential risks to the local community. Thus, the current study uses 42 synoptic meteorological stations to assess the spatiotemporal changes in air temperature over Myanmar during 1971–2013. The nonparametric sequential Mann-Kendall (SqMK), linear regression, empirical orthogonal function (EOF), Principal Component Analysis (PCA), and composite analysis were used to assess the long-term trends in maximum (Tmax) and minimum (Tmin) temperature series and their possible mechanism over the study region. The results indicate that the trend of Tmax has significantly increased at the rates of 90% in summer season, while the Tmin revealed a substantial positive trend in winter season time series with the magnitude of 30%, respectively. Moreover, during a rapid change of climate (1995–2013) we observed an air temperature increase of 0.7 °C. The spatial distributions of EOF revealed relatively warmer temperatures over the whole region except the south in the summer; however, a similar pattern can be seen for the rainy season and winter, implying warming in the central part and cooling in the northern and southern parts. Furthermore, the Indian Ocean Dipole (IOD) influence on air temperature over Myanmar is more prevalent than that of the El Niño Southern Oscillation (ENSO). The result implies that the positive phase of the IOD and negative phase of the Southern Oscillation Index (SOI; El Niño) events led to the higher temperature, resulting in intense climatic extremes (i.e., droughts and heatwaves) over the target region. Therefore, this study's findings can help policymakers and decision-makers improve economic growth, agricultural production, ecology, water resource management, and preserving the natural habitat in the target region.

**Keywords:** air temperature; interannual variability; ENSO; IOD; Myanmar



**Citation:** Mie Sein, Z.M.; Ullah, I.; Syed, S.; Zhi, X.; Azam, K.; Rasool, G. Interannual Variability of Air Temperature over Myanmar: The Influence of ENSO and IOD. *Climate* **2021**, *9*, 35. <https://doi.org/10.3390/cli9020035>

Received: 19 December 2020

Accepted: 16 February 2021

Published: 21 February 2021

**Publisher's Note:** MDPI stays neutral with regard to jurisdictional claims in published maps and institutional affiliations.



**Copyright:** © 2021 by the authors. Licensee MDPI, Basel, Switzerland. This article is an open access article distributed under the terms and conditions of the Creative Commons Attribution (CC BY) license (<https://creativecommons.org/licenses/by/4.0/>).

## 1. Introduction

In a tropical country like Myanmar, air temperature is the most significant weather and climate element and is very useful for living, society, human activities, culture, and traditions [1,2]. Agriculture is a mainstay of Myanmar's economy, contributing 25–30% of national GDP, and about 70% of the rural population relies on it for their livelihood and income [3,4]. The temperature affects crops' yields, the patterns of natural vegetation, the rates of biochemical reactions within organisms, and the energy consumed for heating

and cooling buildings [5,6]. The relative humidity and dew point temperature have been widely used to assess the air's moisture amount indicators [7]. Weather phenomena are the consequence of temperature variations, resulting from variations in the energy balance components. Surface warming is abundant over land due to the less efficient evaporative cooling and lower heat capacity associated with the ocean [8].

The variability of maximum and minimum temperature (hereafter Tmax and Tmin) has more effects on the natural and built environment than mean temperature (Tmean) [3]. It has also been reported that the spatiotemporal variability of Tmax and Tmin have substantially affected the frequency, intensity, duration, and spatial extent of temperature extremes around the globe [9]. Extreme temperatures will lead to more extreme weather events (e.g., droughts, heatwaves, cyclones, and sea-level rise) that could negatively impact the socioeconomic situation (e.g., agriculture, health, water resources, aquaculture, livestock, and the forestry sector) in the region [1,6]. The spatiotemporal variability of seasonal Tmax and Tmin coupling with precipitation can also affect the variability of water for drinking, irrigation, and other domestic purposes [10]. Therefore, the assessment of long-term changes in Tmax and Tmin is vital for understanding the influences of climate change, particularly in agriculture dependent country like Myanmar. A less developing country like Myanmar needs improved knowledge and insightful understanding regarding temperature variations and their effect on agriculture, water scarcity, food security, and temperature extremes [3,11–13]. This information could play a pivotal role in long-term planning for climate change adaptation and disaster risk management at the regional and local levels [14].

Myanmar is located in one of the fast temperature rising zones and hence, highly vulnerable to climate change. Numerous studies have reported dynamic variations in Tmax and Tmin over distinct regions of Myanmar [3,4,15]. Htway et al. (2011) [16] described that the annual Tmax and Tmin are continuously increased over the whole region between mid-April and mid-May. They also reported that the Tmean has increased at the rates of by 0.08 °C per decade, with fewer cold days and more persistently hot days; 15 heatwaves happened in 1951–2000, with the most severe occurring in 1998 during the El Niño Southern Oscillation (ENSO) year in the region [3,4,15]. Similarly, increasing trends were detected in Tmax and Tmin over the entire country at the rates of 0.11 and 0.09 °C per decade, respectively [3]. They also found that the average Tmax of Yangon City is increasing, while the average Tmin has significantly decreased over 60 years, which leads to a decline in daily Tmean decade by decade [17,18]. On the other hand, Myanmar recorded new Tmax as high as 40–45 °C and 37–46.5 °C from April to May in 2010 and 2016, respectively [13]. However, the studies mentioned above have reported significant results with respect to dynamic variability of Tmax and Tmin over Myanmar. Though previous studies were limited to a specific region, low stations density, less temporal coverage, and/or different methodology, from the best of our knowledge none of them considered the dynamic drivers over the diversified climatic region. Therefore, the present study is an improvement in term of the Interdecadal variability of temperature with the extended time scale, high stations density, and potential mechanism. Furthermore, previous research did not investigate fully the potential drivers of air temperature over the study region.

The El Niño Southern Oscillation (ENSO) is the primary mode of interannual variability on the tropical Pacific with significant influences on global weather and climate via atmospheric circulations. Given this, efforts have been made to develop different forecasting methods to predict ENSO evolution several seasons in advance [3,4]. It is well documented in the literature that interannual temperature variability over Myanmar is influenced by several dominant large-scale modes of climate variability [19]. Trenberth et al. (1998) [20] described the large-scale difference of the tropopause as an annual cycle and longer-term interannual variability related to the ENSO. However, ENSO substantially affects the global to regional variability of the air temperature [21–23]. The variability of the climatic conditions in the Indian Ocean (IO) and Pacific Ocean (PO) is influenced by the IOD and the ENSO, both of which have substantial impacts on the climate of Asia [24]. Joseph et al.

(2016) [25] showed that a strong negative IOD was a strong promoter of the weak La Niña of 2016. Thirumalai et al. (2017) [26] observed that Southeast Asia's surface air temperatures exceeded national records in April 2016. This indicates a correlation between ENSO and Southeast Asian surface air temperatures, in that all April extremes occur during El Niño years.

This study aims to explore the interannual variability of air temperature and its possible mechanism over Myanmar. Indeed, Myanmar faces a significant challenge in anticipating, preventing, and proactively reducing disasters' impacts and coping with increasing exposure to high-risk scenarios. A better understanding of the interannual variability of temperature and its possible mechanisms is essential for improved disaster risk management and early warning system planning. Thus, it is crucial to study the interannual variability of temperature's impact of ocean-atmosphere events like IOD and ENSO in the region. The rest of the paper is structured as follows: Sections 2 and 3 describe the study area and methodology, the results and discussion are given in Section 4, and conclusions are presented in Section 5.

## 2. Study Area

Myanmar is located in the Southeast Asia region, with geographical coordinates of  $9^{\circ}32'$  to  $28^{\circ}31'$  N latitude and  $92^{\circ}10'$  to  $101^{\circ}11'$  E longitude (Figure 1). The region is situated between the Indian Ocean and the Bay of Bengal in the west, the Philippine Sea, the South China Sea, and the Pacific Ocean in the east [19]. Myanmar's climate is mostly influenced by the Indian summer monsoon [27–29]. The country has a tropical to subtropical monsoon climate, with three seasons: warm and cool intermonsoonal (mid-February to mid-May); rainy southwest monsoon (mid-May to late October); and cool and warm northeast monsoon (late October to mid-February) (NAPA 2012). Moreover, the region is located in the Indian Monsoon regions, where weather/climate disasters lead to frequent damage in the summer monsoon season (May–October). For example, in 2019 and 2020, extreme floods and landslides occurred in Myanmar due to the strong monsoon precipitation and resulted in considerable loss of life and property. Long-lasting extremely warm periods and a very low amount of total monsoon precipitation (May–October) lead to water scarcity and threaten the economic livelihood and food security in the country [1,30]. Water scarcity occurs in the central warm and deltaic regions during the summer (March–April) [6,31].

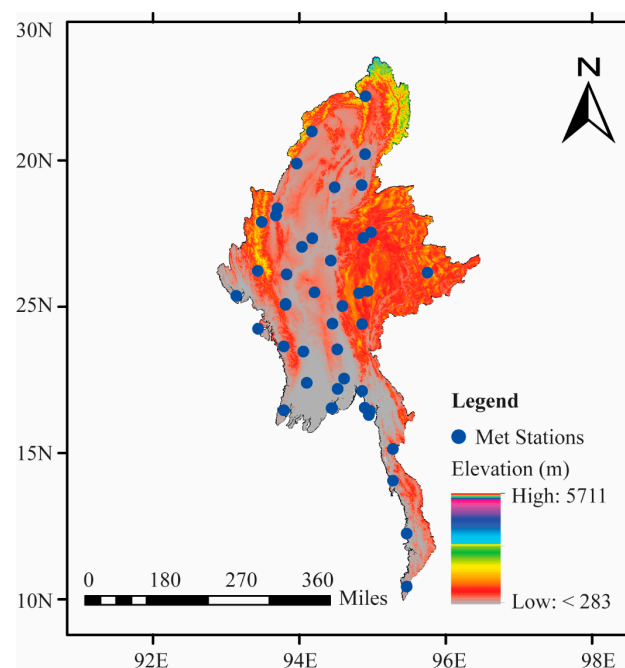


**Figure 1.** Elevation of the study area map with 42 meteorological stations across Myanmar.

### 3. Materials and Methods

#### 3.1. In-Situ Observation

We used the monthly maximum (Tmax), minimum (Tmin), and mean (Tmean) temperature datasets of 42 meteorological stations from 1971 to 2013. The data were obtained from the Department of Meteorology and Hydrology (Myanmar). The details of each meteorological station are presented in Figure 1 and Table S1. The stations' selection was done based on their long-term temporal coverage, data homogeneity, and the data record's completeness. Recent studies have reported that the use of gauge-based gridded data is a good choice for detailed study of distinct climatic factors in the study region [1,30]; however, application of the gridded datasets for similar purposes is subjected to validation to document their strengths and uncertainties [19]. This study considered temperature variations according to the country's seasons based on the summer (March–April), rainy season (May–October), and winter (November–February). Moreover, we also used NCEP/NCAR reanalysis datasets on monthly means of meridional and zonal winds with spatial resolution of  $0.1^\circ \times 0.1^\circ$  [32,33]. The NOAA/OAR/ESRL PSL (Boulder, CO, USA) provided daily relative humidity data from NCEP Global Analyses. Extended Reconstructed SST (ERSST v5) was acquired from the National Oceanic and Atmospheric Administration (NOAA), with grid size resolution of  $0.1^\circ$  at monthly time scale [32]. The Southern Oscillation Index (SOI), East, and west Dipole Mode Index (DMI) monthly datasets were also collected from the NOAA [3,15].

#### 3.2. Methods

This study uses different statistical approaches including Mann-Kendall (MK), sequential Mann-Kendall (SqMK), linear regression, empirical orthogonal function (EOF), Principal Component Analysis (PCA), and composite analysis to assess the spatiotemporal changes in temperature over Myanmar and the influence of ENSO and IOD. The nonparametric MK test was applied to determine the significant trend in temperature, whereas the linear regression was employed to calculate the magnitude of the trend in the selected time scale [1,2,11]. The nonparametric SqMK test was used to detect the abrupt changes or shifts in the temporal trend of temperature over Myanmar. The brief details for MK and SqMK techniques are described in Appendix A. Moreover, EOF analysis was applied to investigate the dominant modes of variability of different seasons (summer, rainy, and winter) air temperature in the target region. EOF is a widely used statistical method to minimize the multidimensionality of complex climate data and identify the most complex physical modes while ensuring that minimal information is lost [34]. Detailed information about EOF analysis is shown in Appendix B. The modes that account for the largest percentage of the original variability are considered significant [35]. These modes can be represented by orthogonal spatial patterns (Eigenvectors) and corresponding time series (PCA).

Furthermore, the composite analysis is carried out to understand the interannual variability of air temperature over the study region. The correlation analysis, which reveals superficial relationships between pairs of variables, is used in this study. The correlation coefficient ( $r$ ) is bounded by  $-1$  and  $1$ ; when the value of  $r$  is  $+1$  or  $-1$ , it indicates a perfect positive or negative correlation between a given pair of variables, respectively [36]. Anomalies are estimated based on the climatology of air temperature for 43 years. Anomaly  $Z$  was computed as expressed in Equation (1):

$$Z = \frac{X - \bar{X}}{S_d}, \quad (1)$$

where  $X$  is the observed air temperature;  $\bar{X}$  is the long term Tmean, and  $S_d$  is the air temperature's standard deviation. The value of  $Z$  presents immediate information about the significance of a particular deviation from the mean [37].

## 4. Results and Discussion

### 4.1. Characteristics of Air Temperature over Myanmar

Generally, Myanmar has three seasons: summer (March–April), the rainy season (May–October), and winter (November–February). Figure 2 shows the spatial spreading of annual average air temperature over Myanmar from 1971 to 2013. The results indicate mixed behavior over the study region, such as  $T_{max}$  ranges from 34.3 °C to 24 °C (Figure 2a),  $T_{min}$  ranges from 23.3 °C to 14.4 °C (Figure 2b), and temperature (mean) ranges from 27.9 °C to 19.6 °C (Figure 2c), respectively. The results further support the findings of [3,4], who reported an abrupt  $T_{mean}$  increase of 0.2 °C in 1993–2010. Myanmar experienced possible further increases in temperature in the warm season, exacerbating drought periods [30]. The high temperatures were seen in the central warm zone (Mandalay, lower Sagaing and Magway regions), west (Rakhine State), and south (Yangon, Bago, Ayeyarwady and Tanintharyi regions, Mon and Kayin States), with cold temperature in the north (Kachin State), northwest (Chin State), and east (Shan state) (Figure 2).

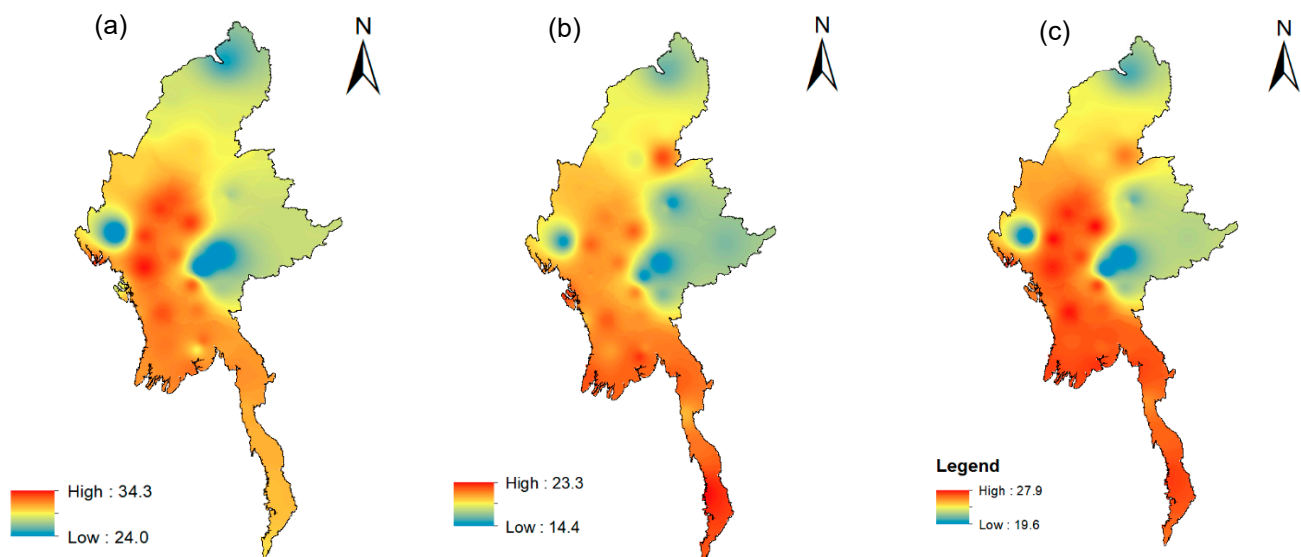


**Figure 2.** Annual average air temperature in the study area (1971–2013). (a) Maximum, (b) minimum, (c) mean.

The annual cycle for temperature that includes  $T_{max}$ ,  $T_{min}$ , and  $T_{mean}$  results is shown in Figure S3. The results analysis revealed that the annual cycle of  $T_{max}$  has its peak in the summer months (March–April), while the lowest point is in the winter (November–February), as seen in Figure S3. The present study results concurred with the previous studies' findings for the target region [38,39]. Horton et al. (2017) observed an average temperature increase of 0.25 °C during 1981–2010; the warming was quicker inland than in coastal areas. The increase in daily  $T_{max}$ s has been more than the daily average constructed on analyses of 19 observed weather stations. The  $T_{min}$  exhibits a peak in the summer and rainy season months (April–October) and a low point in the winter (December–February) (see Figure S1). The results of the present study agree with previous studies' similar findings over Myanmar [38]. However, the  $T_{mean}$  reveals the peak in summer and pre-monsoon periods (April–May) and the lowest point in winter months (December–February), which coincides with the monsoon season (Figure S3).

Figure 3 elucidates the seasonal  $T_{max}$ ,  $T_{min}$ , and  $T_{mean}$  for the summer (March–April), rainy season (May–October), and winter (November–February) across Myanmar in 1971–2013. The results include the seasonal average  $T_{max}$  during 1971–2013 for the summer (35 °C), rainy season (31.1 °C), and winter (29.6 °C) (Figure 3a). Moreover, the  $T_{min}$  is shown for the summer (20.5 °C), rainy season (23.3 °C), and winter (15.8 °C). Moreover, the  $T_{mean}$  is obvious over the study region for the summer (27.3 °C), rainy season (27 °C), and winter (22.7 °C) (see Figure 3b). The country experienced an increase in temperature

variability, and precipitation patterns varied [3,40]. Monthly air temperature (Tmax and Tmin) results for 1971–2013 concerning the normal (Tmax and Tmin) air temperature during 1981–2010 are presented in Figure S2. The results indicated that the Tmax (1971–2013) significantly increased in the summer (March) (Figure S2a). Following the observed diurnal irregularity in the global warming trend, the Tmin increased more quickly than the daytime temperatures [41]. The Tmaxs were continuously high in the whole region during mid-April and mid-May, as reported by [16]. On the other hand, the Tmin (1971–2013) significantly increased each year over study area (Figure S2b), implying that the region was prone to more severe extreme weather events. Furthermore, the Tmax and Tmin (%), based on the average air temperature (1981–2010), further clarifies the results, as shown in Figure S9.

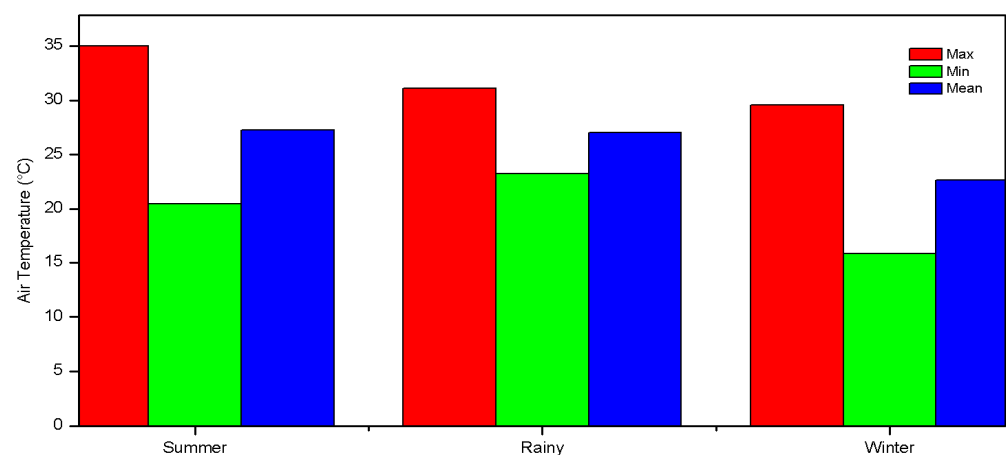


**Figure 3.** Seasonal temperature (maximum, minimum, and mean) for summer (March–April), rainy season (May–October), and winter (November–February) during the period 1971–2013 (in °C).

From the results, it can be inferred that the Tmax is expected to significantly increase (90%) in March, decrease (10%) in July, August, October, and November, decrease (20%) in December, January, and April, and decrease (30%) in February over the study region. Several studies based on observational and reanalysis data have reported severe heatwave, drought, and flood events in the target region in recent decades [5,42–44], highlighting the degree of vulnerability to climate change and climate extremes. Interestingly, the Tmax results for Myanmar increased significantly (90%) in the summer, especially in March. After that, Tmin increased (30%) in November and December, increased (20%) in March–April, September–October, and increased (10%) in January and May–August. The Tmin increased over the whole year in the region, with a particularly significant increase in the winter months (November and December). Surface warming is abundant over land due to the less efficient evaporative cooling and lower heat capacity associated with the ocean [8]. Table S2 shows the difference between the Tmax and Tmin (1971–2013) based on the average air temperature (1981–2010). It can be concluded from the results that the monthly Tmin increased more than the Tmax in the whole year over the target regions. Our results confirm the warming rate reported by [3,4], who employed a high-resolution downscaled model over the target region.

#### 4.2. Interannual Variability of Air Temperature in Myanmar

Figure 4 demonstrates the annual Tmean anomalies and its linear trend over the study area. The interannual variability of the air temperature anomalies trend over Myanmar in 1971–2013 is shown in Figure 4a and is particularly obvious after 2000. Figure 4b indicates the detrended annual mean anomalies of air temperature over the study region, which shows the predominant interannual variability with warm and cold years. During seasonal variability (i.e., summer, rainy season, and winter), warm and cold years are estimated based on the detrended time series of seasonal air temperature over Myanmar (see Table S3).

Oo et al. (2019) [39] studied the seasonal temperature changes analysis for all stations in the Upper Ayeyarwady river basin. They reported that the future temperature is predicted to increase steadily, with higher rates during the summer than in the other two seasons. It can also be determined that the monthly Tmin increase is more than the Tmax rise in all seasons. Warm and cold years are evident in all seasons over the target region; however, a warming trend is more prominent in the target region (Table S3). Here, it is interesting that the year 1998 was drier in all three seasons (summer, rainy season, and winter). The results coincide with the severe heatwaves that occurred in 1998 [42,45]. Moreover, cold years in winters such as 1989 and 2011 were in healthy La Niña years, except for 1992. The years in which air temperature is above (below) one standard deviation appeared as warm (cold) years. These patterns further clarify the analysis of particular composite years to observe further trends (i.e., wind speed, relative humidity, and sea surface temperature).

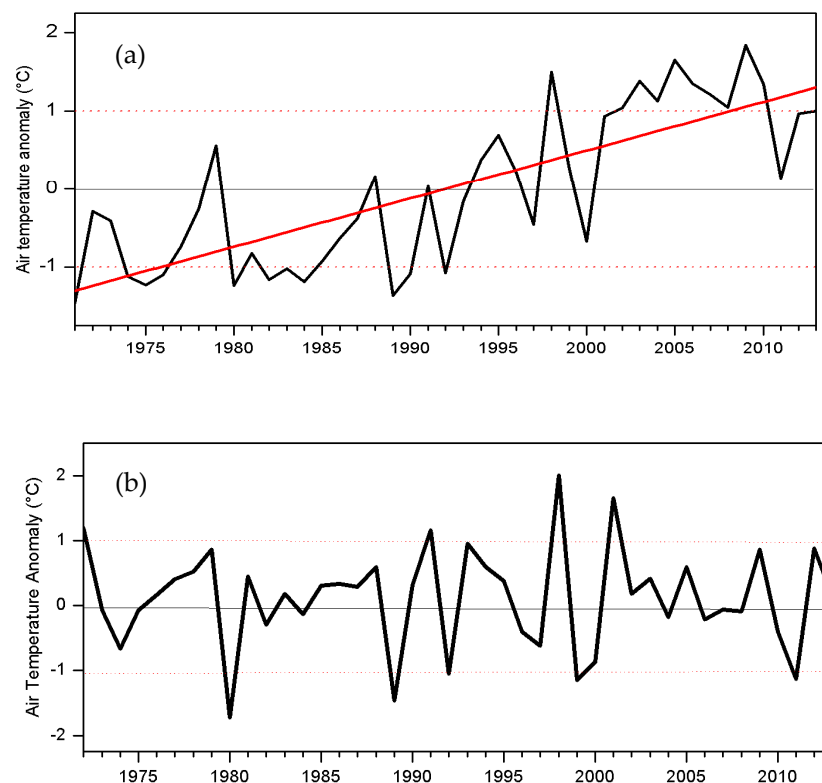


**Figure 4.** (a) Time series of annual mean air temperature anomalies and its linear trend (solid red line); (b) detrended time series of annual mean air temperature anomalies.

#### 4.3. Detection of Abrupt Climate Change in Air Temperature over Myanmar

The MK test results indicate a decrease in the Tmean in 1971–1993 (see Figure 5). After that, the air temperature significantly increased, with an abrupt change during 1994. After the change, there was a remarkable increasing trend, which continued until the end of the study period (2013). The results agreed with previous studies from the study area [3,15]. They reported warming periods starting in Myanmar in 1994. Moreover, the analysis of air temperature before and after the observed abrupt change in climate showed that the Tmean after the abrupt change of climate (1995–2013) increased by 0.7 °C, balanced with the time before (1971–1993) the observed change in 1994 (see Table S4). Additionally, long-term trends in the air temperature variation affect climate change in the region [9].

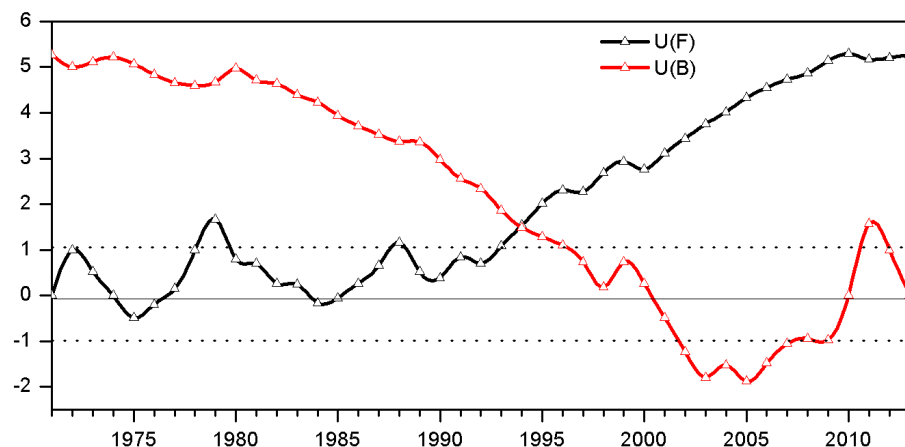
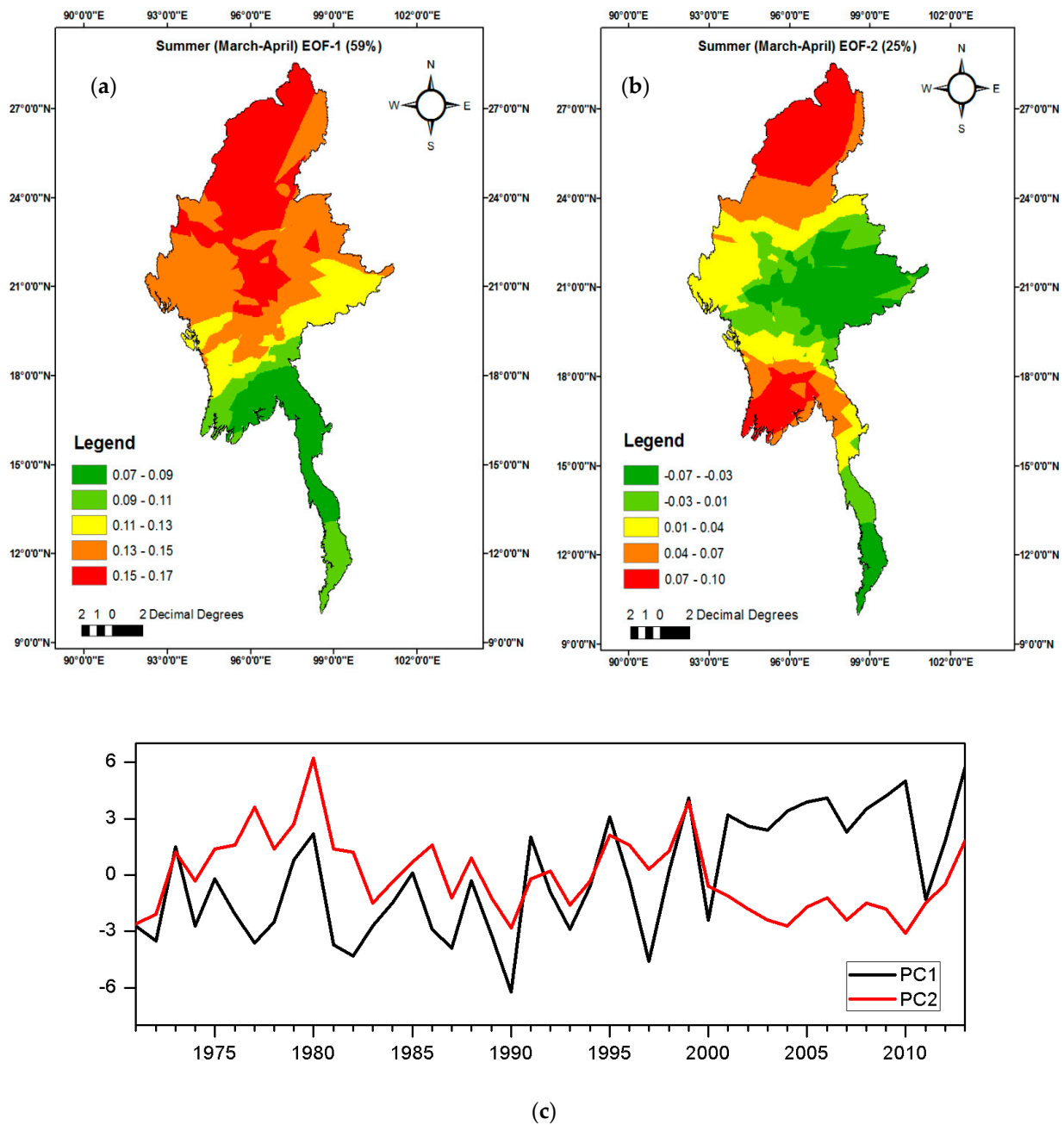


**Figure 5.** Mann-Kendall analysis for annual mean air temperature over Myanmar in 1971–2013. The forward sequential statistic  $U(F)$  is denoted by a solid black line and the backward sequential statistic  $U(B)$  is denoted by a solid red line. The dotted black lines above and below represent significance at the 95% confidence level, and the solid black line marks 0.

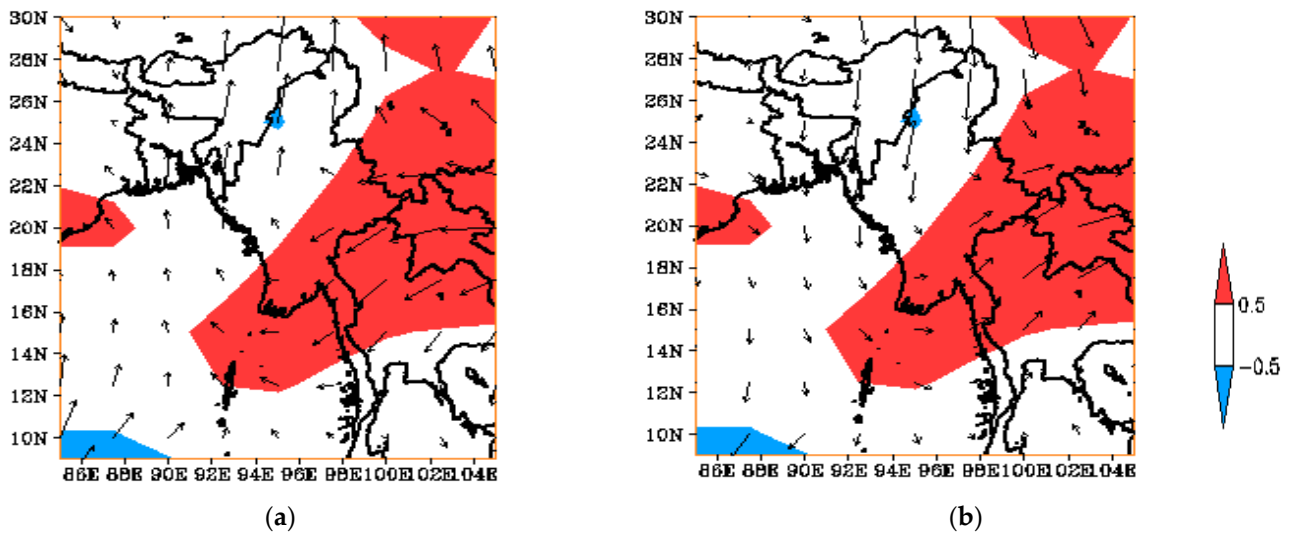
#### 4.4. Dominant Modes in Air Temperature over Myanmar and Possible Causes

The first two dominant modes (EOF-1 and EOF-2) of air temperature are considered for each season (summer, rainy season, and winter) over the study area. Figure 6a shows the EOF-1 spatial pattern of air temperature during the summer, which exhibits a dipole mode with 59% of the total variance, indicating a warming trend in central, eastern, western, and northern parts. In contrast, a cooling pattern was observed in the southern region. The region experienced extreme temperature events in 2010; the warmest year are recorded according to 20 observation stations in 2010 and 56 observation stations in 2016 [1,3,11,19]. Similarly, EOF2 shows a complex pattern (Figure 6b) with a rate of 25% total variance, especially in the central, eastern, and deltaic regions. Principal component (PC) analysis, which is compatible with EOF-1 and EOF-2, is shown in Figure 6c. Warm and cold years are relatively obvious in the PC-1 compared to the PC-2 pattern in the study area.

Figure 7 elucidates the summer (March–April) wind anomaly at 850 hPa for warm and cold years from the composite analysis results over Myanmar (Table S3). The warm years' wind anomaly at 850 hPa indicates a positive anomaly in deltaic, southern, and eastern regions and a prevailing increasing air pattern in the study area, while the northerly winds in the central and northern regions contributed to the northeast winds in the eastern and southern parts (Figure 7a). Our results concurred with previous studies' findings in the target region and neighbouring countries like China and India [1,3,4,11]. They reported that the wind anomaly is higher over the coastal region. During cold years, the wind at 850 hPa shows a positive anomaly in the deltaic, southern, and eastern regions, implying strong wind patterns that favour southerly winds in the central and northern parts of the study area (Figure 7b). Due to soaring day temperatures across the country, cumulonimbus clouds will form, and occasional strong winds happen in the afternoon and evening in the target region. In addition, due to strong annual winds, some areas of Myanmar have already seen strong winds. The increase/decrease in these months and overall variability agree with the regional studies [13,19]. We have recently seen regional impacts, e.g., Mandalay city had strong wind events in April 2013 during which two children died, and at least 12 people were injured because of strong winds in Shan State.

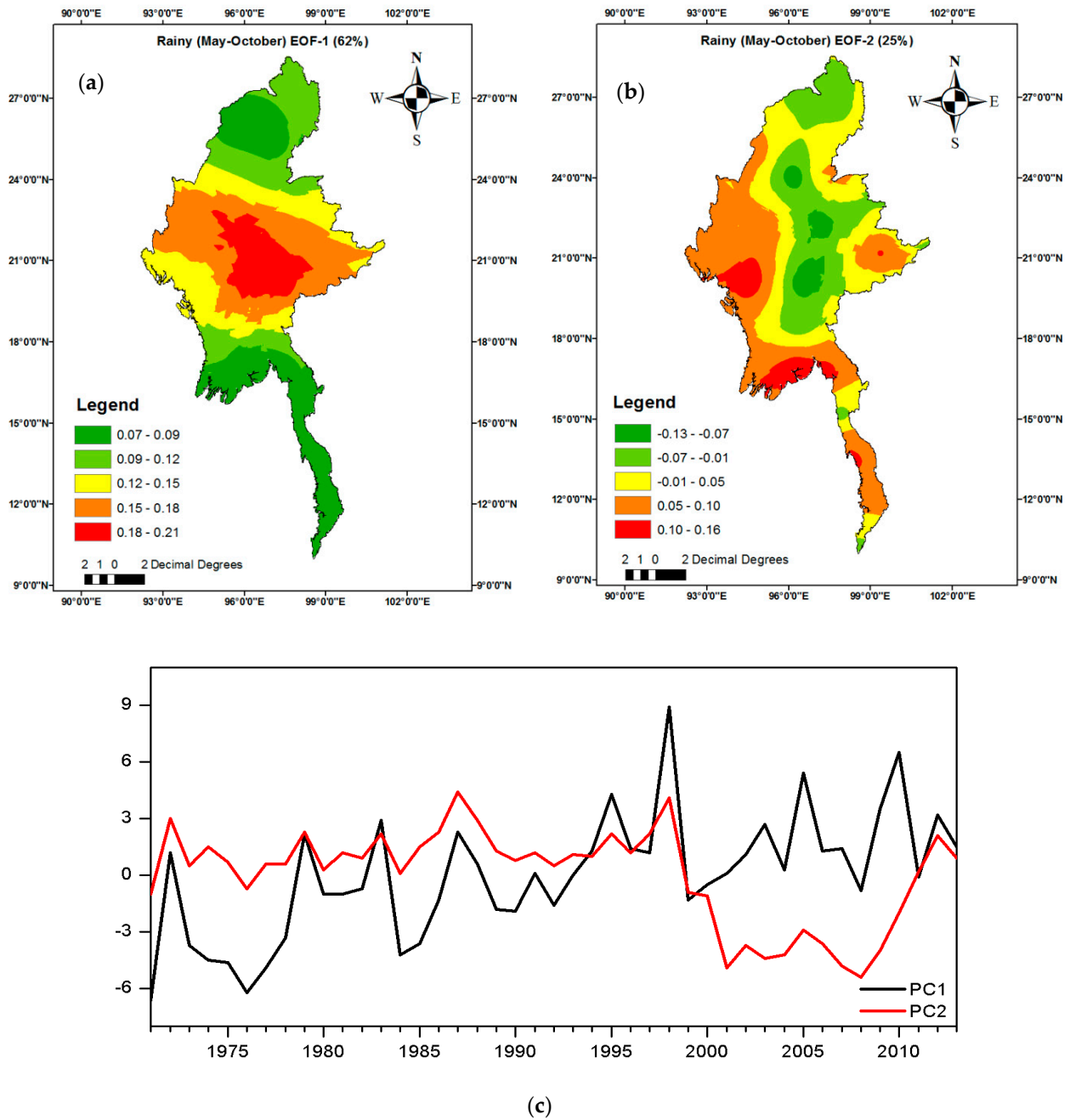


**Figure 6.** Summer season (March-April) air temperature (a), the first mode of EOF (b), and the second mode of EOF (c) indicates the corresponding air temperature principal components of PC1 and PC2.

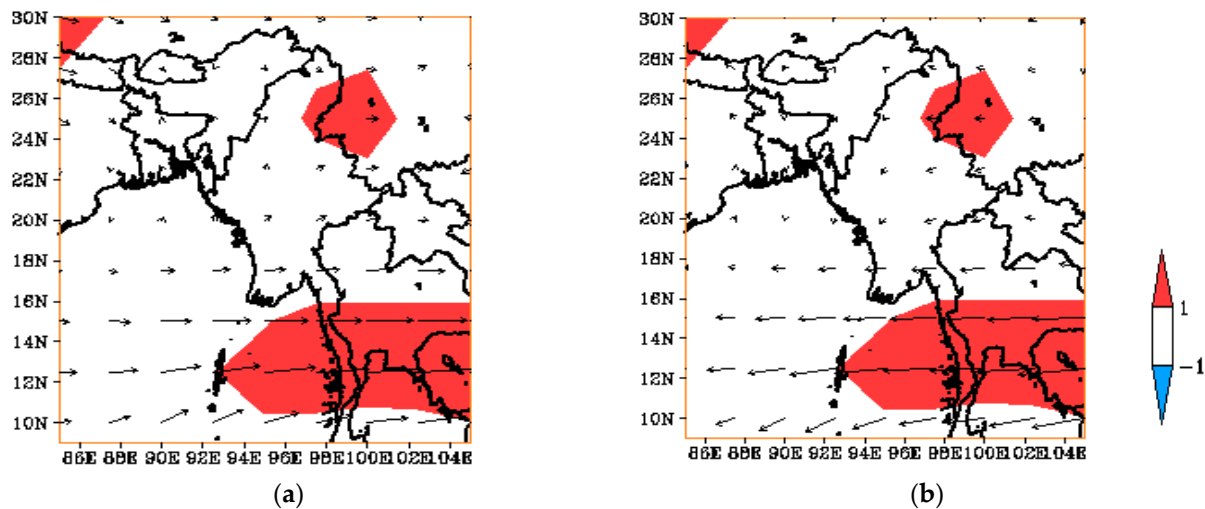


**Figure 7.** Summer (March–April) wind anomaly at 850 hPa for (a) warm years and (b) cold years over Myanmar.

Figure S3 elucidates the difference between warm and cold years in terms of the summer SST anomaly, which tends to be drier in the eastern and central Pacific due to the El Niño pattern related to Myanmar's summer. The difference between warm and cold years in terms of the summer relative humidity (RH) indicates a negative anomaly in the whole region. It is clear that temperature significantly decreases more than RH over the country (Figure 8). Figure 9a shows the dominant modes of variability of the rainy season (May–October) air temperature over Myanmar. The first EOF-1 exhibits 62% of the total variance, a dipole mode pattern of variability with warming in the central warm zone and coldness in the southern and northern regions (Figure 12a). The second EOF-2 spatial pattern explains 25% of the total variance, a dipole mode variability, with warm conditions along the coast and in the northwestern (China State) and eastern (Shan State) regions, whereas increasingly cold weather could be seen in northern, central, and northern Shan State (Figure 9b and Figure S5). It is also anticipated that the spatiotemporal variability of temperature and related extremes will intensify in the near future [39,42]. To some extent, these challenges were associated with large-scale anomalous atmospheric circulation patterns, and the resultant flux resulted in local and remote damage on a vast scale [3,13]. Figure 9a indicates that a rainy season wind anomaly at 850 hPa for cold years leads to westerlies and south westerlies in the region. During cold years, easterlies and northeast winds are dominant in the core regions of the country (Figure 9b). Both warm/cold years appeared to have a positive wind anomaly in southern and northeast regions, with strong westerly winds in warm years; however, a strong easterly wind anomaly was observed during cold years.



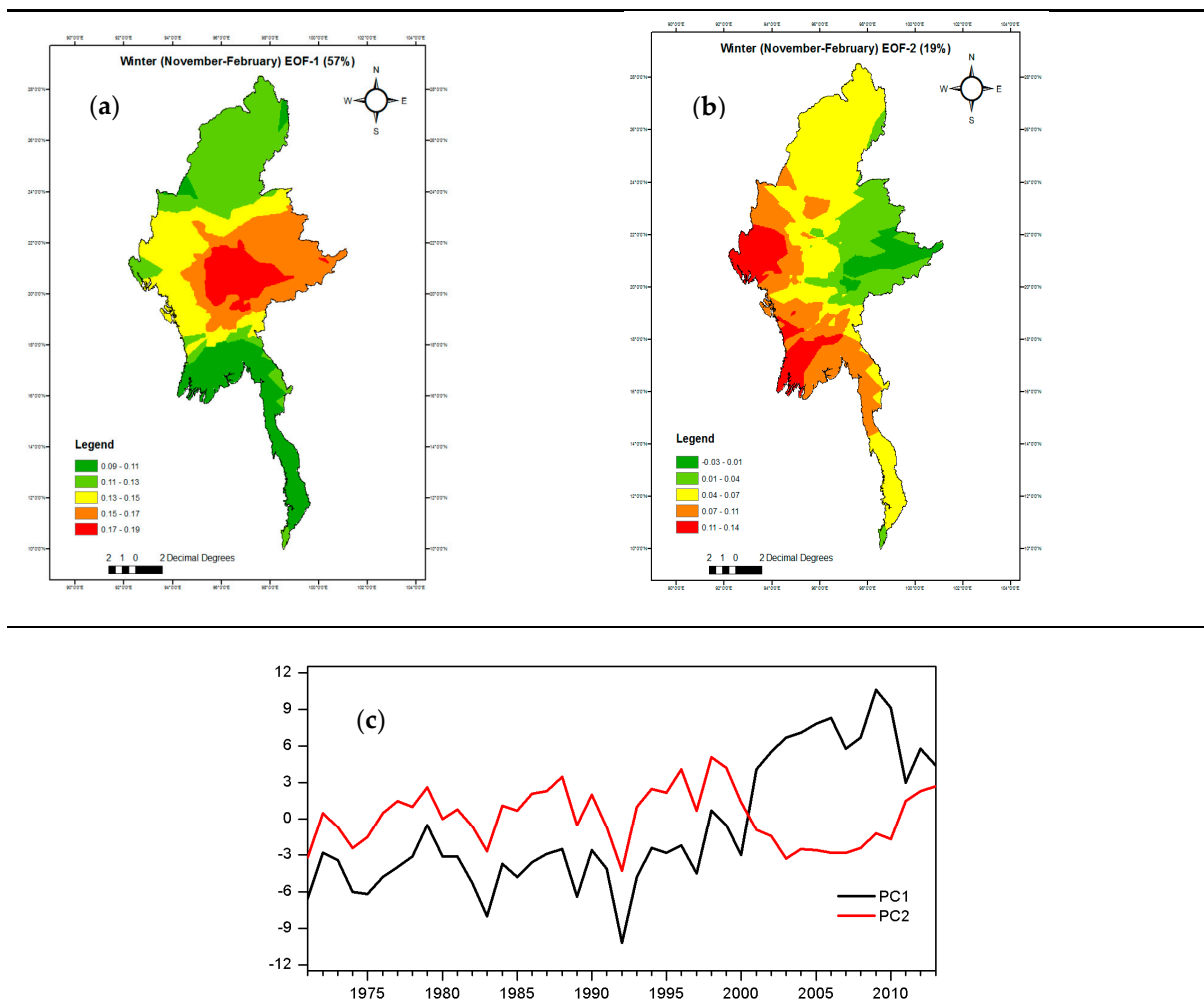
**Figure 8.** Rainy season (May–October) air temperatures (a), the first mode of EOF (b), and the second mode of EOF (c) with respect to corresponding air temperature of principle components (PC1 and PC2).



**Figure 9.** Rainy season (May–October) wind anomaly at 850 hPa for (a) warm years and (b) cold years over Myanmar.

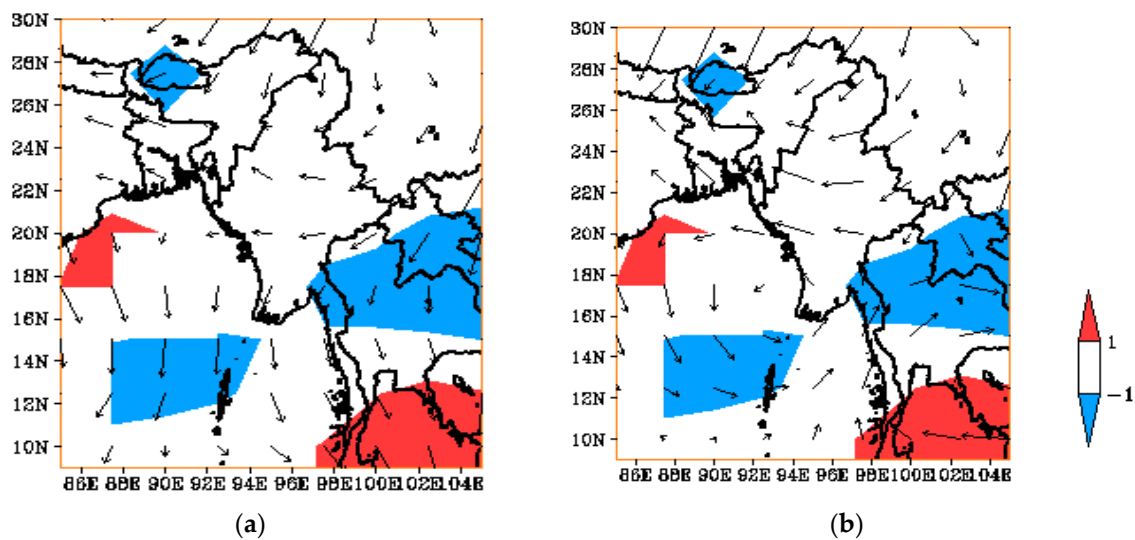
The difference between warm and cold years in terms of the rainy season SST anomaly in the study area is shown in Figure S4. The difference between warm and cold years in the rainy season SST anomaly shows warmer SST in the western Indian Ocean relative to the eastern positive Indian Ocean Dipole (IOD) (see Figure S4). The results indicate that the  $T_{min}$  significantly increased over the region, particularly in the rainy season (Figure S4). Trenberth et al. (1990) described the large-scale difference of the tropopause as an annual cycle and longer-term interannual variability related to the ENSO. They found a significant increase in the target region. Moreover, the relative humidity (RH) anomaly difference for the rainy season in warm and cold years is presented in Figure S6. The results indicate that the difference between warm and cold years in the rainy season of RH anomaly shows a relatively positive anomaly in the southern and eastern parts (see Figure S5), while a negative anomaly was recorded in the western, northwestern, and northern parts of the region (see Figure S6).

The EOF analyses (i.e., EOF-1, EOF-2) for the winter (November–February) compared to the corresponding air temperature of principal components (PC1 and PC2), are presented in Figure 10. Figure 10a elucidates the EOF-1 spatial distribution of air temperature; the results show that the winter explains 57% of the coldness in the region except in the central warm zone and eastern parts. EOF2 of air temperature over Myanmar (Figure 10b) explains 19% of the total variance, with warm weather in the north, west, south of the region, and cool weather in the eastern parts. Both EOF-1 and EOF-2 describe the dipole mode of variability over the target region (Figure 10a,b). Principal components (PC) corresponding to EOF-1 and EOF-2 are shown in Figure 10c. The PC-1 results significantly increase after 2000, implying more temperature intensity in the region.



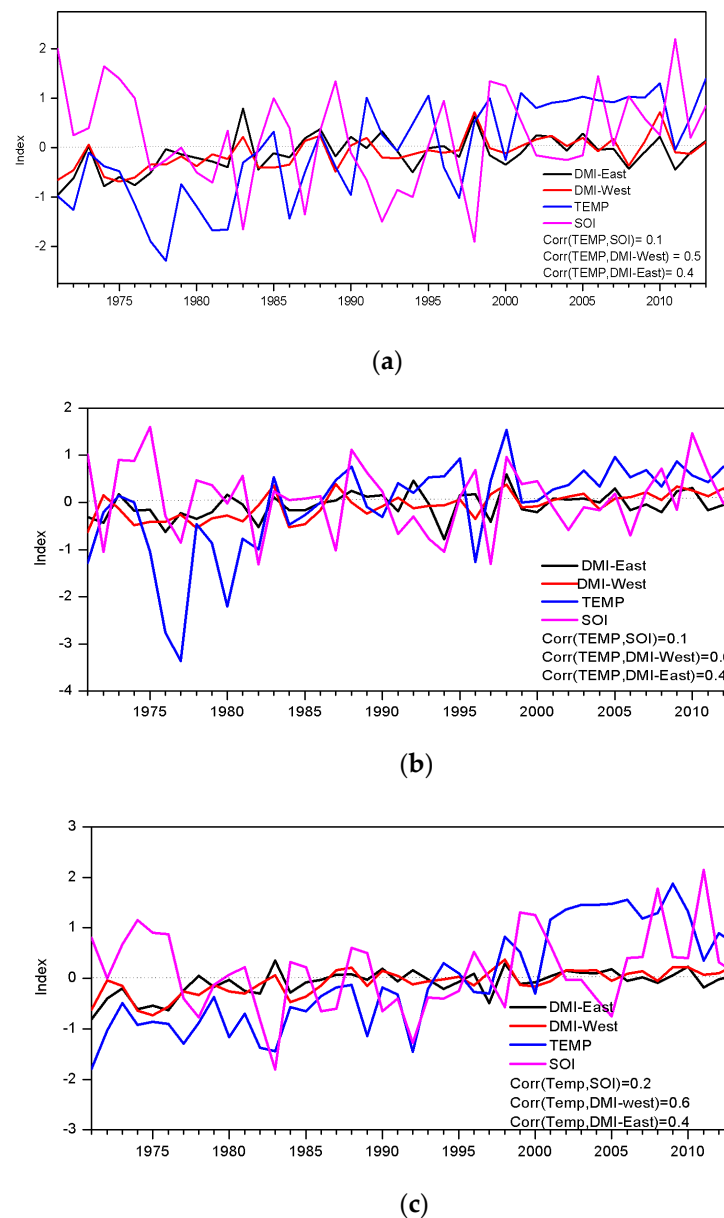
**Figure 10.** Winter (November–February) air temperatures (a), the first mode of EOF (b), and the second mode of EOF (c) with respect to the corresponding air temperature of principal components PC1 and PC2.

Figure 11a indicates the winter wind anomaly at 850 hPa for warm years, which is mainly influenced by easterly and northeast winds in the region. The winter wind anomaly at 850 hPa for cold years encourages northeast winds in the central and northern parts; however, southwest winds in the southern parts show anticyclonic circulation over the east central Bay of Bengal (see Figure 11b). Our results support the findings of [3,11–13], who reported a significant negative anomaly over the region. A negative wind anomaly could be seen for the Mon and Kayin States of the region (see Figure 11). Thirumalai et al. (2017) observed that Southeast Asia’s surface air temperatures exceeded national records in April 2016, indicating a correlation between ENSO and Southeast Asian surface air temperatures. Figure S7 shows the difference between warm and cold years in the winter over the study region. The SST anomaly reveals that the cool weather in the eastern and central Pacific Ocean, as in the La Niña pattern, may be associated with Myanmar’s winter. The difference between warm and cold years in the winter was due to the relative humidity (RH) anomaly, which was largely negative in the central, southern, and eastern parts, while a positive anomaly was recorded over the northwest of the country (see Figure S8).



**Figure 11.** Winter (November–February) wind anomaly at 850 hPa for (a) warm years and (b) cold years in the study region.

Figure 12 shows the interannual variability of the summer monsoon between the Southern Oscillation Index (SOI), the Dipole Mode Index for the west (DMI-West), and the Dipole Mode Index for the east (DMI-East) and the average standardized temperature anomaly in the summer, rainy season, and winter over Myanmar. During the summer, the strong positive correlation of DMI-west (DMI-east) and air temperature over Myanmar was 0.5 (0.4) and the weak positive correlation with SOI and air temperature over Myanmar was 0.1 (see Figure 12a). During the rainy season, the strong positive correlation of DMI-west (DMI-east) and air temperature over Myanmar was 0.6 (0.4) and the weak positive correlation with SOI and air temperature was about 0.1 (see Figure 12b). Moreover, the strong positive correlation of DMI-west (DMI-east) and air temperature over Myanmar was 0.6 (0.4) and a weak positive correlation with SOI and air temperature of around 0.2 was observed in the winter (see Figure 12c). This result implies that the country experiences high temperatures during the positive Indian Ocean Dipole (IOD) and low temperatures during the negative IOD—with low temperatures during positive SOI and high temperatures during negative SOI. During a positive SOI (La Niña year), the air temperature was low over the country; however, a high temperature was reported during negative SOI (El Niño year). Table S5 shows the correlation of seasonal air temperature with the Dipole Mode Index (DMI) and the Southern Oscillation Index (SOI).



**Figure 12.** Interannual variability for (a) summer between Southern Oscillation Index (SOI), Dipole Mode Index (DMI)-West, and DMI-East and average standardized temperature anomaly; (b) rainy season between SOI, DMI-West, DMI-East and average standardized temperature anomaly; and (c) winter between SOI, DMI-West, DMI-East and average standardized temperature anomaly (1971–2013) over Myanmar.

## 5. Conclusions

This study attempted to explore the spatiotemporal trend and variability of seasonal (i.e., summer, rainy, and winter) air temperature during 1971–2013 over Myanmar by using statistical techniques and composite analysis. The study found significant variation in air temperature at interannual and seasonal scale. The summer season observed an increase in mean air temperature magnitude and vice versa for rainy season and winter season. The interannual and seasonal air temperature inferred a westward and northward shift of air temperature maxima from humid to the arid region. At seasonal scale, the interannual air temperature appeared to be subjected to deviation in terms of spread and turning points in trends. It can be remarked that the monthly Tmin has significantly increased compared to the Tmax in the whole study area. Moreover, the assessments of air temperature variability

before and after the observed abrupt change revealed that the Tmean after the abrupt change point (1995–2013) increased by 0.7 °C, as compared with before the change in 1994. In the summer, the leading mode (EOF-1) spatial patterns displayed a dipole mode of about 59% of the total variance, indicating warming in the central, eastern, and northern parts. In contrast, a cooling pattern can be seen in the southern region. The large-scale atmospheric circulation result implies that positive IOD and negative SOI (El Niño) events tend to increase compared to the average air temperature, suggesting extreme events (i.e., droughts and heatwaves) in the region.

Moreover, negative IOD and positive SOI (La Niña) events result in lower than average air temperatures in the region. Therefore, it can be concluded that the ENSO and IOD warming/cooling are leading factors that are responsible for the interannual air temperature variability over Myanmar. Even though the station data is subjected to deviation and uncertainties, the current study has reported diverse variability of the air temperature. Thus, a follow-up study is recommended to model the influence of such indices on temperature variability over Myanmar.

**Supplementary Materials:** The following are available online at <https://www.mdpi.com/2225-1154/9/2/35/s1>, Figure S1. Annual cycle of maximum, minimum, and mean air temperature over Myanmar during 1971–2013; Figure S2. Monthly air temperature in 1971–2013 with respect to normal (maximum and minimum) air temperature (in °C) (1981–2010): (a) maximum and (b) minimum; Figure S3. The difference between warm and cold years for summer SST anomaly; Figure S4. The difference between warm and cold years for rainy season SST anomaly in the study area; Figure S5. The difference between warm and cold years in terms of summer relative humidity anomaly; Figure S6. The difference between warm and cold years for rainy season relative humidity anomaly over Myanmar; Figure S7. The difference between warm and cold years for the winter SST anomaly of the study area; Figure S8. The difference between warm and cold years for the winter relative humidity anomaly; Figure S9. Departure of maximum and minimum air temperature change with respect to normal air temperature (1981–2010) (%); Table S1. Detailed information on the meteorological stations; Table S2. Maximum and minimum monthly air temperature anomalies relative to the normal values averaged over 1981–2010; Table S3. Warm and cold years based on the detrended time series of seasonal air temperature over Myanmar; Table S4. Annual mean temperature showing the long-term mean (1971–2013), the mean values before the change in 1994, and the mean values after the change (1995–2013). Temperature difference means the difference between the mean values (after change minus before change); the observed change in 1994; Table S5. Correlation coefficient of seasonal air temperature with DMI and SOI.

**Author Contributions:** Conceptualization, Z.M.M.S. and I.U., X.Z.; methodology, software, and validation, Z.M.M.S. and I.U.; formal analysis and investigation, X.Z., I.U. and Z.M.M.S.; writing—review and editing, I.U., S.S., and K.A.; data curation, G.R. and Z.M.M.S. All authors have read and agreed to the published version of the manuscript.

**Funding:** This study was supported by the National (Key) Basic R & D Program of China (Grant No. 2012CB955204).

**Data Availability Statement:** All data are available within the manuscript.

**Acknowledgments:** We are grateful to the two anonymous reviewers for their time and support in reshaping the manuscript. Their comments helped us to improve the final version of the manuscript. Furthermore, this research was encouraged by Binjiang College, Nanjing University of Information Science and Technology, Wuxi City, Jiangsu Province, China. Special appreciation goes to the Department of Meteorology and Hydrology, Myanmar, to provide the datasets used in the study.

**Conflicts of Interest:** The authors declare no conflict of interest.

## Appendix A

### *Empirical Orthogonal Function*

Empirical orthogonal function (EOF) analysis was used to investigate the dominant modes of variability of different seasons (summer, rainy, and winter) air temperature over

Myanmar. A similar method has been used in India [9]. The data were normalized to prevent areas of maximum variance from dominating the eigenvectors [35]. EOF is a widely used statistical method to minimize the multidimensionality of complex climate data and identify the most complex physical modes while ensuring that minimal information is lost [34]. It is a commonly used method to draw attention to the physical mechanisms that can potentially contribute to climate variability [46,47]. This technique, also called Principal Component Analysis (PCA), was developed for the analysis of atmospheric data following [48], known as the empirical orthogonal function (EOF) technique [36]. The technique explains the variance and covariance of the data through a few modes of variability. The modes that account for the largest percentage of the original variability are considered significant. These modes can be represented by orthogonal spatial patterns (Eigenvectors) and corresponding time series (principal components). The orthogonal function of EOF is defined in Equation (A1):

$$z(x, y, t) = \sum_{k=1}^N PC(t) \times EOF(x, y), \quad (A1)$$

where  $z(x, y, t)$  denotes the function of space  $(x, y)$ , and time  $(t)$ ; therefore,  $EOF(x, y)$  represents the spatial structure of the temporal variation of  $Z$ .

## Appendix B

### Mann-Kendall Test

The Mann-Kendall test is used to detect trends and abrupt climate change over Myanmar. Mann-Kendall test statistics [49,50] are employed for time series  $x_i$  to detect an event or change points in a long-term time series. The sequential Mann-Kendall test is computed with ranked values,  $y_i$ , of the original values in  $(x_1, x_2, x_3, \dots, x_n)$ . The magnitudes of  $y_i$ , ( $i = 1, 2, 3, \dots, n$ ) are compared with  $y_j$ , ( $j = 1, 2, 3, \dots, j - 1$ ). For each comparison, the cases where  $y_i > y_j$  are counted and denoted by  $n_i$ . The statistic  $t_i$  can, therefore, be defined in Equation (A2):

$$t_i = \sum_{j=1}^i n_i, \quad (A2)$$

The distribution of test statistic  $t_1$  has a mean expressed by Equation (A3):

$$E(t_i) = \frac{i(i-1)}{4}, \quad (A3)$$

and variance as in Equation (A4):

$$Var(t_i) = \frac{i(i-1)(2i+5)}{72}, \quad (A4)$$

The sequential values of a reduced or standardized variable, called statistic  $ut_i$  are calculated for each of the test statistic variables  $t_i$  as follows:

$$U(F) = \frac{([t_i - E(t_i)])}{\sqrt{Var(t_i)}}, \quad (A5)$$

While the sequential forward statistic,  $U(F)$ , is estimated using the original time series  $(x_1, x_2, x_3, \dots, x_n)$ , values of the backward sequential statistic,  $U(B)$  is estimated in the same manner but starting from the end of the series. In determining  $U(B)$ , the time series changes so that the last value of the original time series comes first  $(x_1, x_2, x_3, \dots, x_n)$ . The later version of the Mann-Kendall test statistic allows for detection of the approximate beginning of a developing trend. When the  $U(F)$  and  $U(B)$  curves were plotted, the intersections of the  $U(F)$  and  $U(B)$  curves locate approximate potential trend turning points. If the intersection of  $U(F)$  and  $U(B)$  occurs beyond  $\pm 1.96$  (5% level) of the standardized statistic,

a detectable change at that point in the time series can be incidental. The method has been successfully used globally in trend analysis [4,11,51].

## References

1. Suman, M.; Maity, R. Southward shift of precipitation extremes over south Asia: Evidences from CORDEX data. *Sci. Rep.* **2020**, *10*, 6452. [[CrossRef](#)]
2. Kumar, S.; Hazra, A.; Goswami, B.N. Role of interaction between dynamics, thermodynamics and cloud microphysics on summer monsoon precipitating clouds over the Myanmar Coast and the Western Ghats. *Clim. Dyn.* **2014**. [[CrossRef](#)]
3. Sein, K.K.; Chidthaisong, A.; Oo, K.L. Observed Trends and Changes in Temperature and Precipitation Extreme Indices over Myanmar. *Atmosphere* **2018**, *9*, 477. [[CrossRef](#)]
4. Sein, Z.M.M.; Zhi, X. Interannual variability of summer monsoon rainfall over Myanmar. *Arab. J. Geosci.* **2016**, *9*, 469. [[CrossRef](#)]
5. Dutta, R. Drought Monitoring in the Dry Zone of Myanmar using MODIS Derived NDVI and Satellite Derived CHIRPS Precipitation Data. *Sustain. Agric. Res.* **2018**. [[CrossRef](#)]
6. Omer, A.; Zhuguo, M.; Zheng, Z.; Saleem, F. Natural and anthropogenic influences on the recent droughts in Yellow River Basin, China. *Sci. Total Environ.* **2020**, *704*, 135428. [[CrossRef](#)]
7. Lawrence, M.G. The Relationship between Relative Humidity and the Dewpoint Temperature in Moist Air: A Simple Conversion and Applications. *Bull. Am. Meteorol. Soc.* **2005**, *86*, 225–234. [[CrossRef](#)]
8. Sutton, R.T.; Dong, B.; Gregory, J.M. Land/sea warming ratio in response to climate change: IPCC AR4 model results and comparison with observations. *Geophys. Res. Lett.* **2007**. [[CrossRef](#)]
9. Chowdary, J.S.; John, N.; Gnanaseelan, C. Interannual variability of surface air-temperature over India: Impact of ENSO and Indian Ocean Sea surface temperature. *Int. J. Climatol.* **2014**, *34*, 416–429. [[CrossRef](#)]
10. Asia-Pacific Mountain Network Building resilience of mountain communities to climate change- Asia. *Cambio Clim. Adapt. Retroceso Glaciares* **2008**, *2*, 3.
11. Faustin Katchele, O.; Ma, Z.G.; Yang, Q.; Batebana, K. Comparison of trends and frequencies of drought in central North China and sub-Saharan Africa from 1901 to 2010. *Atmos. Ocean. Sci. Lett.* **2017**, *10*, 418–426. [[CrossRef](#)]
12. Roy Bhowmik, S.K.; Durai, V.R. Multi-model ensemble forecasting of rainfall over Indian monsoon region. *Atmosfera* **2008**, *21*, 225–239.
13. Kreft, S.; Eckstein, D.; Melchior, I. Global Climate Risk Index 2017. Who Suffers Most from Extreme Weather Events? Weather-related loss events in 2015 and 1996 to 2015. *Think Tank Res.* **2017**, *76*, 1–28.
14. IPCC. *Summary for Policymakers—Global Warming of 1.5oC, an IPCC Special Report*; IPCC: Geneva, Switzerland, 2018; ISBN 9783540773405.
15. Sein, M.M.Z.; Ogwang, B.A.; Ongoma, V.; Ogou, F.K.; Batebana, K. Inter-annual variability of Summer Monsoon Rainfall over Myanmar in relation to IOD and ENSO. *J. Environ. Agric. Sci.* **2015**, *4*, 28–36.
16. Htway, O.; Matsumoto, J. Climatological onset dates of summer monsoon over Myanmar. *Int. J. Climatol.* **2011**. [[CrossRef](#)]
17. Oo, S.S.; Hmwe, K.M.; Aung, N.N.; Su, A.A.; Soe, K.K.; Mon, T.L.; Lwin, K.M.; Thu, M.M.; Soe, T.T.; Htwe, M.L. Diversity of Insect Pest and Predator Species in Monsoon and Summer Rice Fields of Taungoo Environs, Myanmar. *Adv. Entomol.* **2020**. [[CrossRef](#)]
18. Rao, M.; Htun, S.; Platt, S.G.; Tizard, R.; Poole, C.; Than, M.; Watson, J.E.M. Biodiversity Conservation in a Changing Climate: A Review of Threats and Implications for Conservation Planning in Myanmar. *Ambio* **2013**, *42*, 789–804. [[CrossRef](#)] [[PubMed](#)]
19. Kreft, S.; Eckstein, D. *Global Climate Risk Index 2014. Who Suffers Most from Extreme Weather Events*; Germanwatch: Bonn, Germany, 2016; ISBN 9783943704143.
20. Trenberth, K.E. Recent observed interdecadal climate changes in the Northern Hemisphere. *Bull. -Am. Meteorol. Soc.* **1990**. [[CrossRef](#)]
21. Kiladis, G.N.; Diaz, H.F. Global Climatic Anomalies Associated with Extremes in the Southern Oscillation. *J. Clim.* **1989**. [[CrossRef](#)]
22. Halpert, M.S.; Ropelewski, C.F. Surface Temperature Patterns Associated with the Southern Oscillation. *J. Clim.* **1992**. [[CrossRef](#)]
23. Kothawale, D.R.; Munot, A.A.; Kumar, K.K. Surface air temperature variability over India during 1901-2007, and its association with enso. *Clim. Res.* **2010**. [[CrossRef](#)]
24. Joseph, P.V. Role of Ocean in the Variability of Indian Summer Monsoon Rainfall. *Surv. Geophys.* **2014**. [[CrossRef](#)]
25. Lim, E.P.; Hendon, H.H. Causes and Predictability of the Negative Indian Ocean Dipole and Its Impact on la Niña during 2016. *Sci. Rep.* **2017**. [[CrossRef](#)]
26. Thirumalai, K.; DInezio, P.N.; Okumura, Y.; Deser, C. Extreme temperatures in Southeast Asia caused by El Niño and worsened by global warming. *Nat. Commun.* **2017**. [[CrossRef](#)] [[PubMed](#)]
27. Sen Roy, N.; Kaur, S. Climatology of monsoon rains of Myanmar (Burma). *Int. J. Climatol.* **2000**. [[CrossRef](#)]
28. Mie Sein, Z.M.; Islam, A.R.M.T.; Maw, K.W.; Moya, T.B. Characterization of southwest monsoon onset over Myanmar. *Meteorol. Atmos. Phys.* **2015**. [[CrossRef](#)]
29. Burki, T. Floods in Myanmar damage hundreds of health facilities. *Lancet* **2015**, *386*, 843. [[CrossRef](#)]
30. Kreft, S.; Eckstein, D. Global Climate Risk Index 2014: Who suffers most from extreme weather events? Weather-related loss events in 2012 and 1993 to 2012. *Ger. Brief. Pap.* **2013**, *28*.

31. Omer, A.; Elagib, N.A.; Zhuguo, M.; Saleem, F.; Mohammed, A. Water scarcity in the Yellow River Basin under future climate change and human activities. *Sci. Total Environ.* **2020**, *749*, 141446. [CrossRef] [PubMed]
32. Huang, B.; Angel, W.; Boyer, T.; Cheng, L.; Chepurin, G.; Freeman, E.; Liu, C.; Zhang, H.M. Evaluating SST analyses with independent ocean profile observations. *J. Clim.* **2018**. [CrossRef]
33. Ullah, I.; Ma, X.; Yin, J.; Asfaw, T.G.; Azam, K.; Syed, S.; Liu, M.; Arshad, M.; Shahzaman, M. Evaluating the meteorological drought characteristics over Pakistan using In-situ observations and reanalysis products. *Int. J. Climatol.* **2021**, j7063. [CrossRef]
34. Hannachi, A.; Jolliffe, I.T.; Stephenson, D.B. Empirical orthogonal functions and related techniques in atmospheric science: A review. *Int. J. Climatol.* **2007**, *27*, 1119–1152. [CrossRef]
35. Walsh, J.E.; Mostek, A. A quantitative analysis of meteorological anomaly patterns over the United States, 1900–1977. *Mon. Weather Rev.* **1980**. [CrossRef]
36. Wilks, D.S. *Statistical Methods in the Atmospheric Sciences*, 2nd ed.; Elsevier: Amsterdam, The Netherlands, 2007; ISBN 9780127519661.
37. Kabanda, T.A.; Jury, M.R. Inter-annual variability of short rains over northern Tanzania. *Clim. Res.* **1999**. [CrossRef]
38. Zin, E.E.; Aung, L.L.; Zin, E.E.; Theingi, P.; Elvera, N.; Aung, P.P.; Han, T.T.; Oo, Y.; Skaland, R.G. Myanmar Climate Report. *Norwegian Meteorological Inst.* **2017**, 105.
39. Oo, H.T.; Zin, W.W.; Thin Kyi, C.C. Assessment of Future Climate Change Projections Using Multiple Global Climate Models. *Civ. Eng. J.* **2019**, *5*, 2152–2166. [CrossRef]
40. Enfield, D.B.; Mestas-Nuñez, A.M.; Trimble, P.J. The Atlantic multidecadal oscillation and its relation to rainfall and river flows in the continental U.S. *Geophys. Res. Lett.* **2001**. [CrossRef]
41. Davy, R.; Esau, I.; Chernokulsky, A.; Outten, S.; Zilitinkevich, S. Diurnal asymmetry to the observed global warming. *Int. J. Climatol.* **2017**. [CrossRef]
42. NECC. *MECF Myanmar's National Adaptation Programme of Action (NAPA) to Climate Change*; NECC: Haverhill, MA, USA, 2012; p. 126.
43. Ko, M.; Kyaw, K.; Aye, N.; Thant, A.A. Drought Analysis for Ayeyarwady Basin. Available online: [https://d1wqtxts1xzle7.cloudfront.net/60027700/pdf20190716-52601-16l3i7v.pdf?1563295069=&response-content-disposition=inline%3B+filename%3DDrought\\_Analysis\\_for\\_Ayeyarwady\\_Basin.pdf&Expires=1613969561&Signature=duXItJG6FheDDGqbbD2BOq4Bxw4zky1x9hjaPFxcR69bLC3s~{}W27tcwdT3JWgQ2Ubft8-sASePcqmrBF-ebr4~{}KW0oE5w5JBvnQ5xPARC~{}oHVUHQymlK1AW57-7VTgcvUwML7SU2hvvfv6UgbAkcEluBgiUM77zGR8Ho18rSXiaedP6cThPcdh~{}1VhPEnNjyxb29s9yWbpUfj~{}PYVix1afrS-nYmry1ZxSGLzmTMO8T8I2ospZMlphr7u1q6kuTrke-rcMmwZbb5gZa4x~{}YIO9xW2nFaDv7E0y9Cf0kyZNf4CHnKHZiksmQSqic~{}kxRzvUaurwaLC0Efb9y9zbVQ0w\\_\\_&Key-Pair-Id=APKAJLOHF5GGSLRBV4ZA](https://d1wqtxts1xzle7.cloudfront.net/60027700/pdf20190716-52601-16l3i7v.pdf?1563295069=&response-content-disposition=inline%3B+filename%3DDrought_Analysis_for_Ayeyarwady_Basin.pdf&Expires=1613969561&Signature=duXItJG6FheDDGqbbD2BOq4Bxw4zky1x9hjaPFxcR69bLC3s~{}W27tcwdT3JWgQ2Ubft8-sASePcqmrBF-ebr4~{}KW0oE5w5JBvnQ5xPARC~{}oHVUHQymlK1AW57-7VTgcvUwML7SU2hvvfv6UgbAkcEluBgiUM77zGR8Ho18rSXiaedP6cThPcdh~{}1VhPEnNjyxb29s9yWbpUfj~{}PYVix1afrS-nYmry1ZxSGLzmTMO8T8I2ospZMlphr7u1q6kuTrke-rcMmwZbb5gZa4x~{}YIO9xW2nFaDv7E0y9Cf0kyZNf4CHnKHZiksmQSqic~{}kxRzvUaurwaLC0Efb9y9zbVQ0w__&Key-Pair-Id=APKAJLOHF5GGSLRBV4ZA) (accessed on 19 December 2020).
44. Zin, W.W.; Kawasaki, A.; Hörmann, G.; Acierto, R.A.; San, Z.M.L.T.; Thu, A.M. Multivariate flood loss estimation of the 2018 bago flood in Myanmar. *J. Disaster Res.* **2020**. [CrossRef]
45. De, U.; Dube, R.; Rao, G. Extreme weather events over India in the last 100 years. *J. Indian Geophys. Union* **2005**.
46. Dommenges, D.; Latif, M. A cautionary note on the interpretation of EOFs. *J. Clim.* **2002**. [CrossRef]
47. Baldwin, M.P.; Stephenson, D.B.; Jolliffe, I.T. Spatial weighting and iterative projection methods for EOFs. *J. Clim.* **2009**. [CrossRef]
48. Lorenz, E.N. Empirical Orthogonal Functions and Statistical Weather Prediction. *Tech. Rep. Stat. Forecast Proj. Rep. 1 Dep. Meteorol. MIT 49* **1956**.
49. Mann, H.B. Nonparametric Tests Against Trend. *Econometrica* **1945**. [CrossRef]
50. Kendall, M.G. *Rank Correlation Methods*, 4th ed.; Griffin: Spokane, WA, USA, 1957.
51. Nalley, D.; Adamowski, J.; Khalil, B.; Ozga-Zielinski, B. Trend detection in surface air temperature in Ontario and Quebec, Canada during 1967–2006 using the discrete wavelet transform. *Atmos. Res.* **2013**. [CrossRef]